ACS OMEGA

http://pubs.acs.org/journal/acsodf

Article

FRET-Based Genetically Encoded Sensor to Monitor Silver Ions

Neha Agrawal, Neha Soleja, Reshma Bano, Rahila Nazir, Tariq Omar Siddiqi, and Mohd Mohsin*

Cite This: *ACS Omega* 2021, 6, 14164–14173

Read Online

ACCESS | Metrics & More | Article Recommendations | Supporting Information

ABSTRACT: Silver is commonly used in wound dressing, photography, health care products, laboratories, pharmacy, biomedical devices, and several industrial purposes. Silver (Ag^+) ions are more toxic pollutants widely scattered in the open environment by natural processes and dispersed in soil, air, and water bodies. Ag^+ binds with metallothionein, macroglobulins, and albumins, which may lead to the alteration of various enzymatic metabolic pathways. To analyze the uptake and metabolism of silver ions in vitro as well as in cells, a range of high-affinity fluorescence-based nanosensors has been constructed using a periplasmic protein *CusF*, a part of the CusCFBA efflux complex, which is involved in providing resistance against copper and silver ions in *Escherichia coli*. This nanosensor was constructed by combining of two fluorescent proteins (donor and acceptor) at the N- and C-terminus of the silver-binding protein (*CusF*), respectively. SenSil (WT) with a binding constant (K_d) of 5.171 μM was more efficient than its mutant variants (H36D and F71W). This nanosensor allows monitoring the level of silver ions in real time in prokaryotes and eukaryotes without any disruption of cells or tissues.

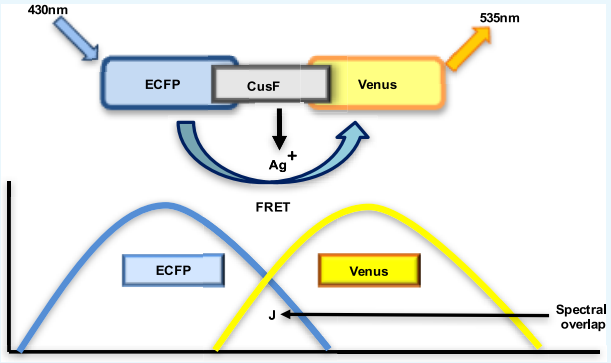

1. INTRODUCTION

Various metals have direct or indirect impact on living organisms. They are required as an essential nutrient in very low concentrations for diverse physiological and biochemical functions in the body. High dose of these heavy metals can be noxious and causes adverse effects on human health. Metal toxicity is a major threat for environment as well as for living organisms. Various metals like lead, arsenic, nickel, silver, and copper have delirious effects and can cause chronic toxicity in humans.[1] Because of the versatile use of silver in biomedical applications, silver toxicity has become a major concern. Silver is a white lustrous transition metal having minor toxicity in humans.[2] Due to several anthropogenic activities, free silver ions are present in the human body at minor concentrations through inhalation of environmental pollutants but do not have trace metal value in the human body. Intentional use of silver in medical devices, dental products, antibacterial and antifungal agents, cosmetics, and wound and burn care products increases the potential exposure of silver ions.[3] Lately, silver usage has led to concerns about the safety aspects and potential risks of the biologically active Ag^+ ion exposure in the environment and human body.[4] Nowadays, silver combined with sulfadiazine provides a broader spectrum of antimicrobial agents.[10] Metallic silver and inorganic silver compounds ionize in aquatic environments and release biologically active Ag^+ ions. These active Ag^+ ions compete with the kinetics of water hydrates and readily bind and precipitate with organic and inorganic cations, which increase acute silver toxicity. Current studies suggest that less than 10% of the silver toxicity occurs by human ingestion,[5] but this is highly variable depending on age, health, nutritional status, and dietary composition. Individuals who are vulnerable to prolonged silver exposure suffer from allergic reactions, irritation in the respiratory tract, and blue-gray staining of the skin (argyria). Studies conducted on severely argyric patients indicate that the amount of silver absorbed by the human body is low but 18% of it is retained in the body, which causes the discoloration of tissues.[6]

Presently, toxic risks by ingestion of silver with food and drinking water are low. But direct inhalation of silver fumes/dust, medicinal uses and occupational exposure trigger the absorption of Ag^+ ions through the gastrointestinal tract and these silver particles accumulate in the bones, kidneys, liver, and skin tissues.[7] Due to its antimicrobial properties, silver is also used as silver copper filters in the water purification process instead of chlorine in hospitals and burn clinics. Industrial workers who have long-term exposure to free silver ions have shown increased concentrations in the hair, blood, urine, and feces.[8,9] Because of their interaction with various biological molecules, intercellular proteins, and inactivating sulfhydryl group of enzymes, Ag^+ ions can cause cytopatho-

Received: February 9, 2021
Accepted: April 29, 2021
Published: May 27, 2021

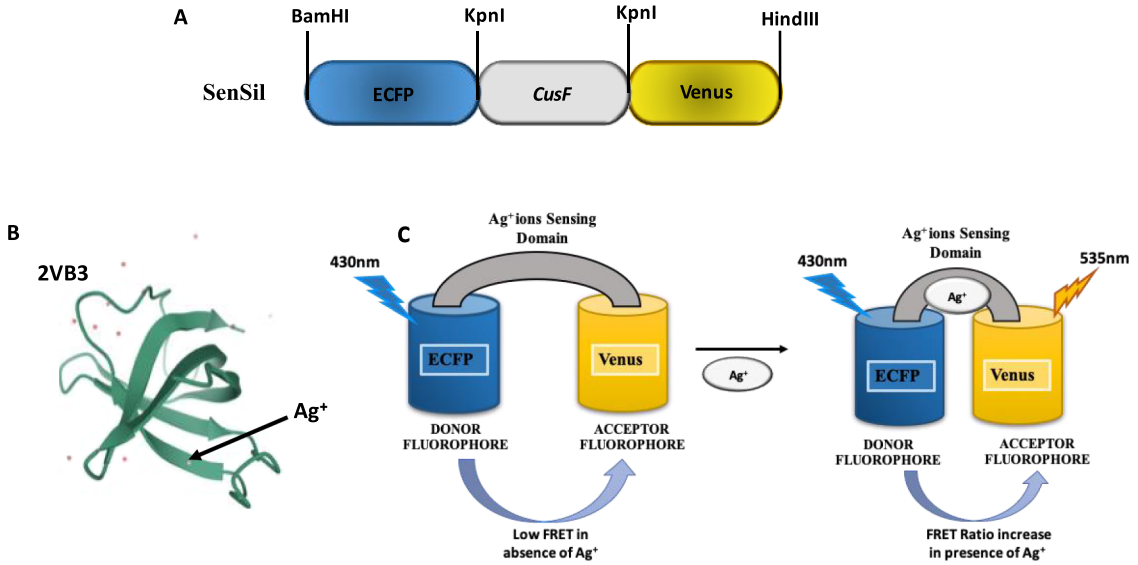

Figure 1. (A) Construction of the FRET-based genetically encoded sensor for silver ions. (B) Crystal structure of *CusF*. (C) Energy transfer illustration in the absence (left) and presence (right) of the Ag^+ ligand.

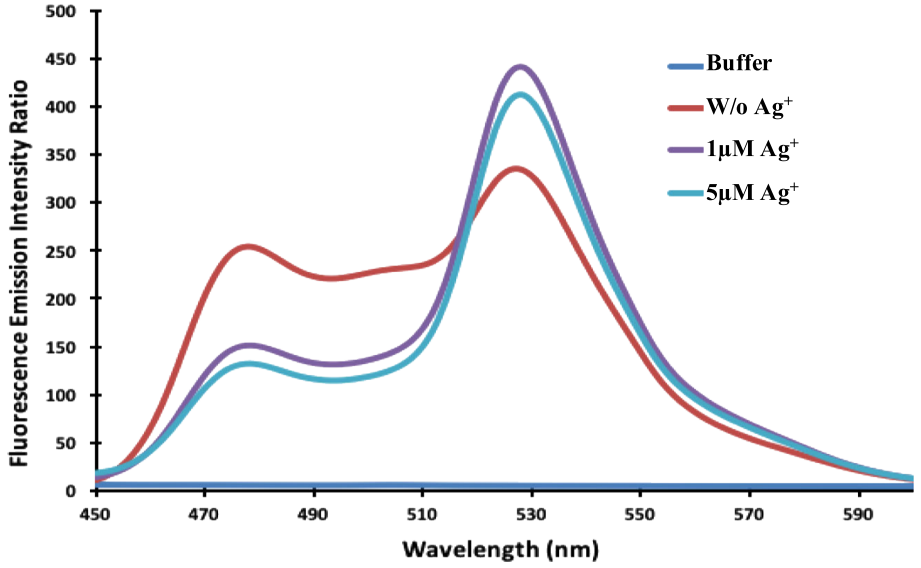

Figure 2. Spectral analysis of the FRET-based nanosensor. The emission spectrum was recorded after excitation of the sensor protein at 420 nm and recording the emission in the range of 450 to 600 nm both in the absence and presence of silver ions.

genic effects on cells and tissues like human gingival fibroblasts, keratinocytes, and endothelial cells.[10,11] Clinical and experimental studies indicate that prolonged exposure of metallic silver ions or ionizable silver compounds may cause bone toxicity, renal toxicity, carcinogenicity, infertility, and impaired fetal growth.[12] Traditional methods for quantification of Ag^+ ions include atomic absorption spectrometry,[13] inductively coupled plasma-mass spectrometry,[14] and ion-selective electrode.[15] However, the expensive instrumentation, invasive nature, and less selectivity and sensitivity limit the applications of these traditional methods.[16,17] Thus, creating a rapid and simple alternative method for the detection of Ag^+ ions in real time is highly desirable. A range of fluorescence-based biosensors has been developed for monitoring silver ions in real samples. A C−Ag^+−C structure-based fluorescence biosensor has been developed by Li et al. (2019)[18] for the detection of Ag^+ ions in real samples of lake water and human sera. They used a C−Ag^+−C structure with signal amplification using an Exo III-assisted dual-recycling process for the synthesis of the biosensor. Ustimova et al. (2018)[19] developed a Förster resonance energy transfer (FRET)-based chemosensor for ratiometric detection of metal ions including silver ions. This sensor has a crown with a bisstyryl dye in which oxocrown ether (donor) transfers the energy to the azadithiacrown ether (acceptor). Although such sensors for measuring silver ions are in practice, but analytical problems of standardization, reproducibility, sample preparation, and analysis make them more cumbersome to use. Organic dyes used in biosensors are vulnerable to metabolic degradation. Because of these degradations, they have least photostability. These dyes have reduced the quantum yield and showed small Stokes shift.[20] On the contrary, we have used various mutant variants of green fluorescent protein as a substitute for these toxic dyes to limit their drawbacks. Fluorescence-based

https://doi.org/10.1021/acsomega.1c00741
ACS Omega 2021, 6, 14164−14173

genetically encoded nanosensor is an efficient device for quantifying the level of metabolites in prokaryotes and eukaryotes noninvasively. However, a FRET-based genetically encoded sensor has not been developed for monitoring silver ions at the cellular level in real time. Therefore, we have created a range of fluorescence-based genetically encoded biosensors for the quantification of Ag^+ ions in cells. Our study suggests that this analytical method has great potential and is able to monitor the flux of Ag^+ ions in real time.

2. RESULTS AND DISCUSSION

2.1. Generation of the Nanosensor. *CusF* was used to construct a genetically encoded FRET-based nanosensor for monitoring the silver ions. For designing FRET nanosensors, ECFP (donor) and Venus (acceptor) fluorophores were used, which are the most promising fluorescent pair among the various variants of fluorescent proteins.[21] Signal peptides were eliminated, the nucleotide sequence of the *Cus*F gene was introduced between the ECFP (donor) and Venus (acceptor) gene sequences for the construction of SenSil, and this sequence was further shuttled in various expression vectors. A linear diagram shows the position of the restriction sites in the nanosensor construct (Figure 1A,B). The proximity changes in emission spectra of both fluorophore proteins in ligand bound and unbound states are shown in Figure 1C. The FRET efficiency largely depends on the dipole orientation, proximity distance between the donor and acceptor fluorophores (10−100 Å), and emission intensity overlap between the donor and acceptor fluorophore proteins.

2.2. Expression and Purification of the Sensor Protein. The sensor plasmid was transformed and expressed in *Escherichia coli* (*E. coli*) BL21 (Codon Plus strain). Chimeric protein (SenSil) was successfully purified by His-tag-based Ni-NTA agarose resin affinity chromatography and confirmed by SDS-PAGE. This purified protein was used for in vitro study of the nanosensor protein.

2.3. Emission Spectra of SenSil. The emission spectral analysis showed a shift in the emission spectrum of fluorescent proteins in the absence and presence of silver ions. In the absence of silver, no changes occur in the emission spectrum. The shift in the spectrum was observed by adding different concentrations (1 and 5 μM) of silver ions (Figure 2). The emission spectral profile of ECFP (donor) and Venus (acceptor) shows respective change in the emission intensities with the addition of silver ions. On increasing the silver ion concentration, major conformational changes occur in the *CusF* protein that brings the two fluorophores close enough to transfer the maximum energy from ECFP to Venus. Thus, the emission intensity of ECFP decreases and the emission intensity of Venus increases subsequently.[22] The binding of silver ions to the periplasmic binding protein (PBP) introduces conformational changes, which led to the fluorophore pairs to come in close proximity of <10 nm, and ultimately fulfills the requirements of FRET to occur.

2.4. Testing the pH Stability of SenSil. The purified nanosensor protein was characterized in vitro in various buffer systems at diverse pH values ranging from 5.0 to 8.0. Among the various buffer systems used, the constructed nanosensor showed the maximum stability in the 3-*N*-morpholino propane sulfonic acid (MOPS) buffer as least changes in the ratio were observed with this buffer (Figure 3A). For further analysis, the sensor protein was diluted in the MOPS buffer. To evaluate the pH stability of SenSil, the FRET ratio was recorded in the

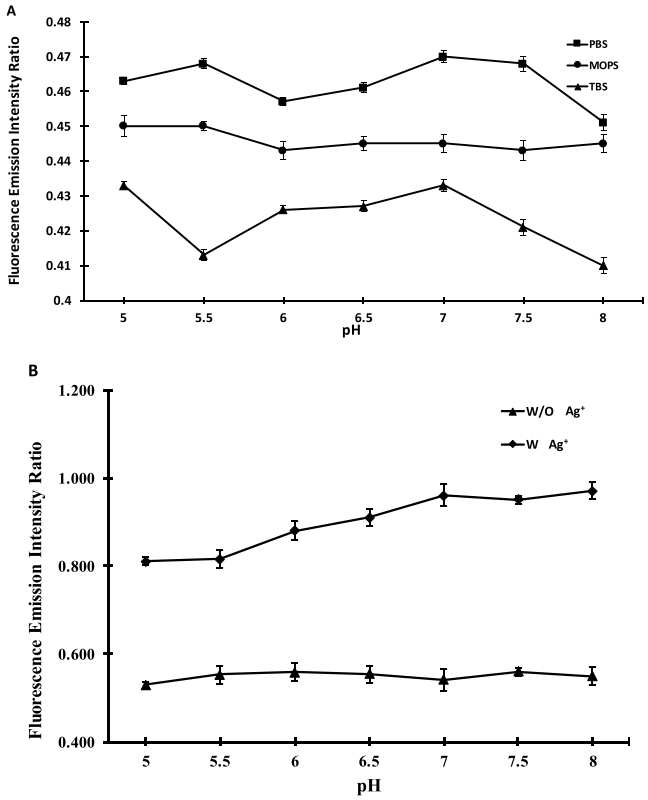

Figure 3. Buffer stability analysis of SenSil. (A) Emission intensity ratio was recorded in MOPS, phosphate-buffered saline (PBS), and Tris−Cl buffer with various ranges of pH values. The sensor was found to be stable in 20 mM MOPS buffer as least change in the FRET ratio was observed with this buffer. (B) Stability of the nanosensor was analyzed in MOPS buffer in a physiological pH range (5.0 to 8.0) in the absence and presence of 1 μM silver ions. Data are means of three independent replicates (n = 3). Vertical bars indicate the standard error.

physiological pH range (5.0−8.0). Addition of 1 μM Ag^+ ion to the purified protein resulted in substantial changes in the FRET ratio up to pH 6.0, suggesting the sensitivity of the sensor protein in the acidic range, while no significant change occurred in the FRET ratio above pH 7.0, confirming the stability of the nanosensor in the alkaline pH range (Figure 3B). The stability of the genetically encoded nanosensor in cytosolic and intracellular pH makes it more compatible for monitoring the silver ions in living systems.

2.5. Specificity and Effect of Metal Ions. In vitro specificity analysis of SenSil was performed using a microplate reader by taking silver, manganese, iron, copper, and nickel at different concentrations, 100, 200, and 500 nM and 1, 5, and 10 μM each. A significant change in the FRET ratio was observed with the addition of 10 μM concentration of silver ions, when compared to control (no silver) (Figure 4A). The effect of biological metal ions (Na^+, K^+, Ca^{2+}, and Mg^{2+}) on the specificity of the nanosensor protein was also observed by recording the FRET ratio (540/485 nm) after mixing 180 μL of diluted protein with 20 μL of physiological concentration of these biological metal ions. No significant changes were observed in the FRET ratio with these metal ions, which shows the efficacy of SenSil toward silver ions (Figure 4B). FRET-based nanosensors open a window for the PBPs. These nanosensors are the most suitable candidates for the ligand-sensing domain, which bind with specific substrates.[23] The

https://doi.org/10.1021/acsomega.1c00741
ACS Omega 2021, 6, 14164−14173

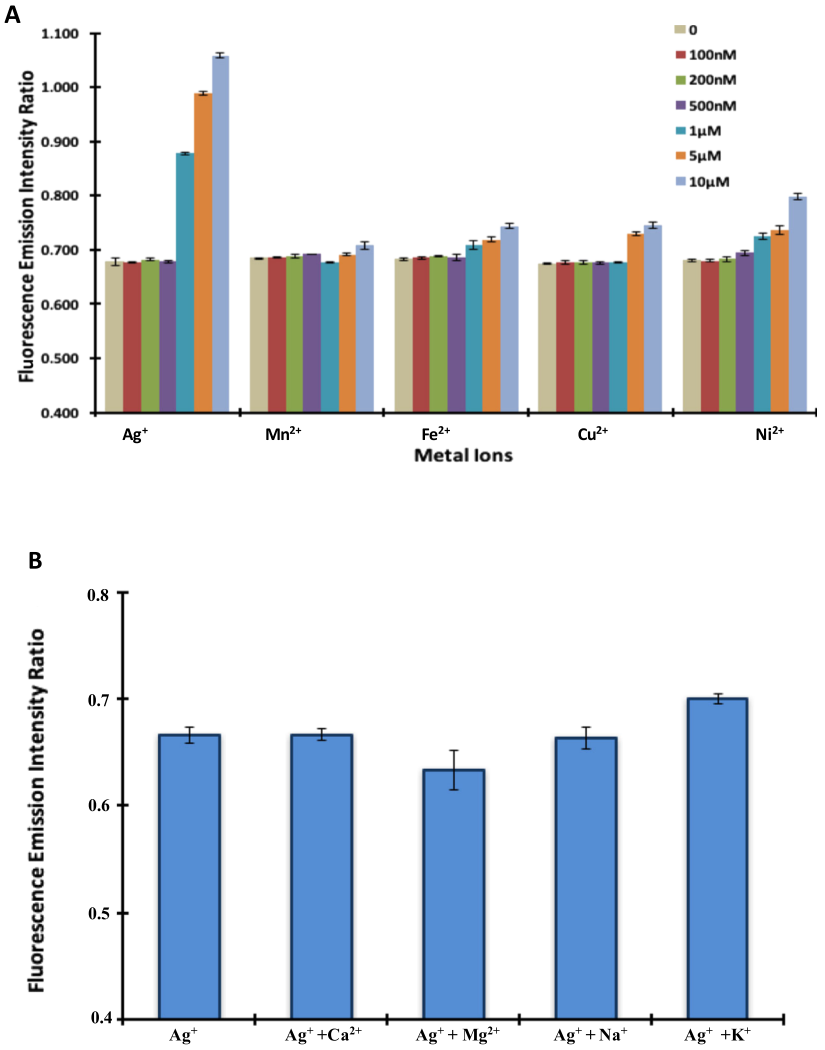

Figure 4. In vitro specificity analysis of SenSil. (A) Specificity of the sensor protein was confirmed by measuring the FRET ratio in the presence of different metal ions (Ag^{+}, Mn^{2+}, Fe^{3+}, Cu^{2+}, and Ni^{2+}). (B) Effect of essential metal ions such as NaCl, KCl, $CaCl_2$, and $MgCl_2$ on the efficiency of the nanosensor, which does not interfere with the specificity of SenSil. Data are means of three independent replicates (n = 3). Vertical bars indicate the standard error.

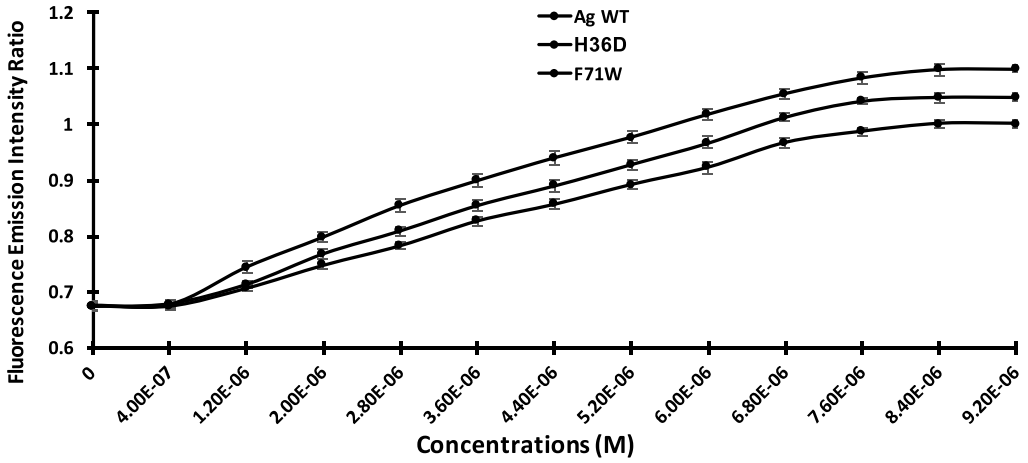

Figure 5. In vitro ligand-dependent FRET emission change of WT and mutant sensors in the presence of different silver ion concentrations. Affinity mutants H36D and F71W were created and compared with the WT sensor protein. Data are means of three independent replicates (n = 3). Vertical bars indicate the standard error.

hinge-bend movement of these proteins is responsible for major conformational changes. These hinge-like motions transform into ratiometric changes in the emission intensities of the two fluorophores. Other molecules did not show any

https://doi.org/10.1021/acsomega.1c00741
ACS Omega 2021, 6, 14164−14173

significant change in the FRET ratio, suggesting that the sensor is specific for silver ions.

2.6. Saturation Curve and Affinity Variants of SenSil. The saturation curve of SenSil was calculated by conducting the FRET measurements with silver ion concentrations in the range of 0.1−9 μM. In response to the Ag^+ ion, a sigmoid saturation curve was obtained that initially represents the maximum change in the emission intensity ratio from 0.678 to 1.068 till 7 μM Ag^+ ion concentration and further saturated at 7−9 μM (Figure 5). The affinity range of the nanosensor variants was determined by calculating the binding constant (K_d). All readings were taken in triplicate using a microplate reader and SenSil was found to bind with Ag^+ ion with an affinity of 5.171 μM. To expand the physiological range of SenSil, a set of sensor variants was generated by introducing point mutations using site-directed mutagenesis in the binding motif of the protein. Two affinity mutants (H36D and F71W) were formed by replacing the amino acid residues.[24] Affinity of the purified chimeric sensor protein toward different concentrations of silver was determined using a microplate reader. The data show that the mutants H36D and F71W have low affinity toward silver compared to the wild-type (WT) sensor (Table 1). The calculated K_d values of the variants

Table 1. Binding Affinity Constants and Dynamic Range of SenSil-WT and Its Affinity Variants[a]

sensor name[b]	sequences	K_d (μM) (±SD[d])	dynamic range[c] (μM)
Sensil	wild type	5.171 (±0.003)	1.679−7.198
Sensil-36	H36D	5.799 (±0.001)	2.039−6.879
Sensil-71	F71W	5.914 (±0.001)	2.232−7.249

[a]Binding constants were determined in vitro. [b]Number next to the mutant name stands for the position in which the point mutation was created in the sensor variants. [c]Effective quantification ranges between 10 and 90% saturation of the nanosensor. [d]Standard deviation (SD).

H36D and F71W were found to be 5.799 and 5.914 μM, respectively. Based on the affinity constant values, SenSil (WT) has the least K_d value; thus, the WT nanosensor was selected and considered the most efficient tool for the study of the dynamic flux of Ag^+ ions at the cellular level in both prokaryotes and eukaryotes.

2.7. Monitoring of SenSil in Bacteria and Yeast. For the determination of the function of SenSil in a cellular system, the sensor was expressed in the cytosol of bacterial cells. The suspension of the expressed *E. coli* BL21 (DE3) bacterial cells was tested in the presence and absence of silver ions. Metabolite accumulation and measurement were also carried out earlier using the FRET-based genetically encoded sensor in prokaryotes.[25] With the addition of 5 μM silver, changes in the FRET ratio occur significantly. No significant change in the FRET ratio was observed in the absence of silver ions. The FRET ratio of the cell suspension increased distinctly with silver after 5 min and saturated at 55 min (Figure 6). Bacterial cells containing pRSET-ECFP_*CusF*_Venus were grown to express the sensor protein and images were taken that showed the successful expression of the nanosensor.

For real-time live cell imaging of SenSil in a yeast cell, a construct was transformed in *Saccharomyces cerevisiae* (*S. cerevisiae*) BY4742. For the expression of the sensor protein in yeast, cells were grown in a synthetic defined (SD) growth medium for 3−5 days in the presence of 2% sucrose and 3% galactose as a carbon source and an inducer, respectively. Live cell imaging of *S. cerevisiae*/URA3 strain BY4742 showed the expression of SenSil in the cytosol of the cell, and major portion of the cell remaining unstained indicates the large vacuole area. Yeast cells were then incubated with 5 μM Ag^+ and a change in the emission intensity ratio was monitored for 10 min using LAS-AF software of the confocal microscope. Expressing yeast cells showed a change in the fluorescence intensity of ECFP and Venus (Figure 7A). Ratiometric images of the yeast cell were also acquired while recording the graph that indicated changes within the cell (Figure 7B). The fluorescent nanosensor responded to the changing level of silver, thus allowing the characterization of silver uptake with a subcellular resolution. Previously Fehr et al.[26] have successfully characterized live cell imaging using FRET-based nanosensors to monitor the flux of maltose yeast cells (FLIPmal).

2.8. Monitoring of SenSil in Mammalian Cells. Human embryonic kidney (HEK-293T) cells were used as an experimental eukaryotic system for the characterization of the silver nanosensor. SenSil was transiently transfected into mammalian HEK-293T cells and confocal imaging of the cells was performed after 2−3 days of transfection for better

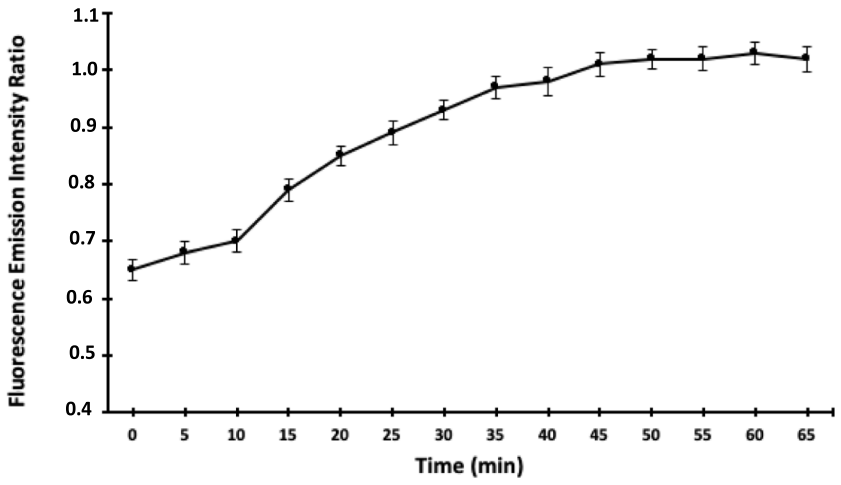

Figure 6. Cell-based analysis of the nanosensor. FRET ratio changes in bacterial cells containing SenSil were recorded in response to 5 μM silver in a time-dependent manner. Data are means of three independent replicates (n = 3). Vertical bars indicate the standard error.

https://doi.org/10.1021/acsomega.1c00741
ACS Omega 2021, 6, 14164−14173

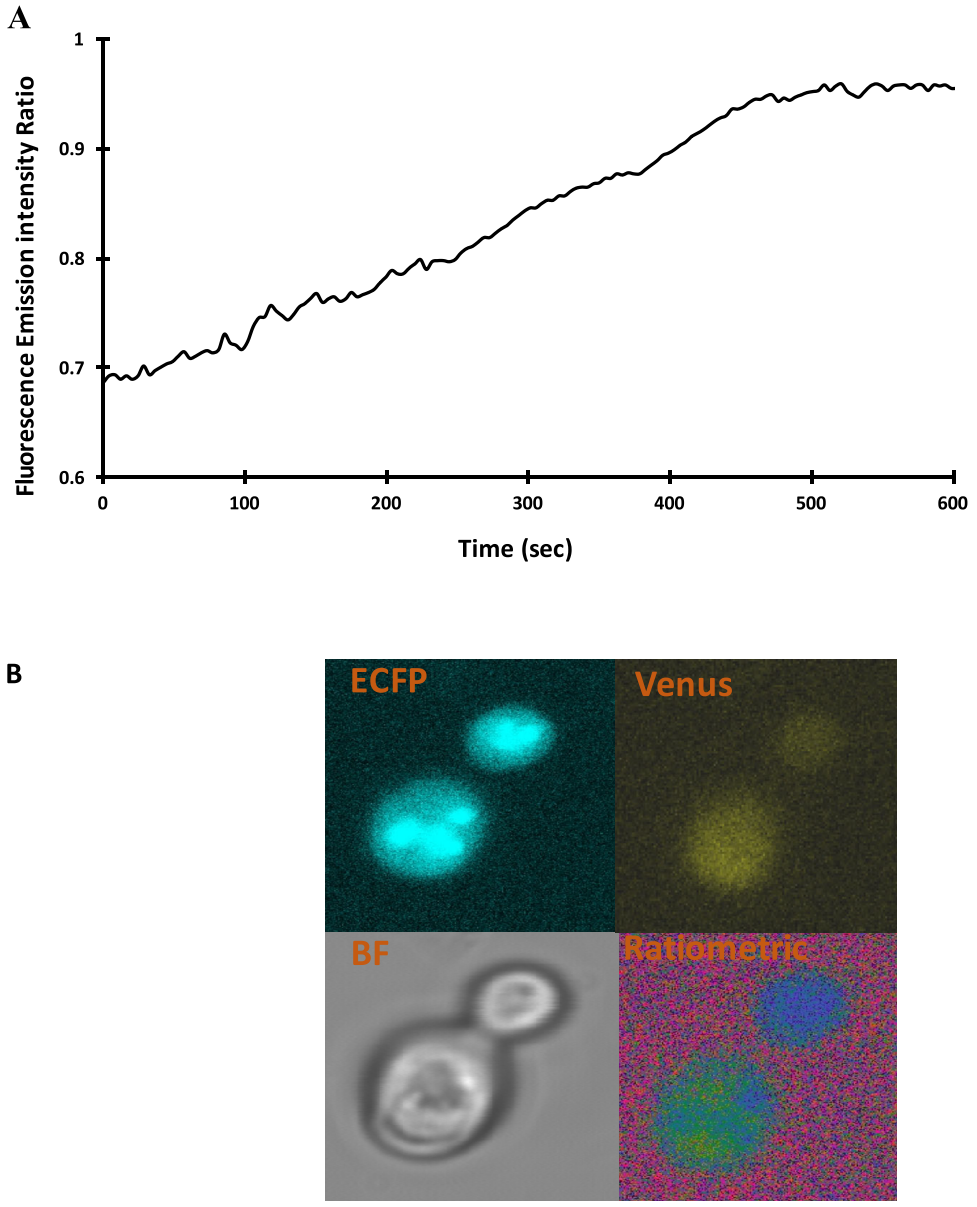

Figure 7. Real-time quantification of the dynamic flux rate change of Ag^+ uptake in yeast cells. (A) The graph indicates change in the FRET ratio in the cytosol of yeast cells in the presence of 5 μM Ag^+ along with the ratiometric changes in a single cell. Change in the FRET ratio indicates the import and binding of Ag^+ ions with SenSil. (B) Confocal images showing cytosolic expression of SenSil in the presence of Ag^+ ions in yeast (*S. cerevisiae*).

expression of the sensor using a Leica microscope acquired at different channels (Figure 8B). The flux of silver ions was monitored noninvasively in the eukaryotic system. With the addition of silver ions, change in the FRET ratio was observed. The emission intensity of Venus increased and that of ECFP decreased in a time-dependent manner. The change in the emission intensity ratio was recorded in a 0−10 min interval, which showed a constant increase with the addition of 5 μM of silver ions (Figure 8A). This sensor has excellent potential to be applied for the real-time monitoring of silver ions in eukaryotic cells without disrupting the cells. It has been previously reported that genetically encoded FRET-based nanosensors have prominent capacity to detect and monitor metabolites such as metal ions in cellular and subcellular components of a mammalian cell, as shown in the case of intracellular fluctuations of second messenger cAMP.[27]

2.9. Cytotoxic Studies. The toxicity of silver ions is not well documented but several recent in vitro cytotoxicity studies demonstrate that Ag^+ ions have the ability to react with sulfhydryl groups, other protein residues, and enzymes, which are associated with cell membranes leading to denaturation, structural damage, and mitochondrial dysfunction.[28] Cultured cells exposed to silver ions showed an altered cell shape and showed evidence of oxidative stress and increased lipid peroxidation.[29] Thus, the cytotoxicity of silver ions cannot be ignored. To determine the in vivo cytotoxicity of silver ions, cell viability studies were carried out. Cell toxicity studies were carried out in a 0−20 μM concentration range of silver ions. It was found that the treatment of Ag^+ does not show significant toxicity to HEK-293T cells in the studied concentration range for 24 h exposure (Figure 8C). The cell viability result showed that treatment of silver becomes toxic at higher concentrations

https://doi.org/10.1021/acsomega.1c00741
ACS Omega 2021, 6, 14164−14173

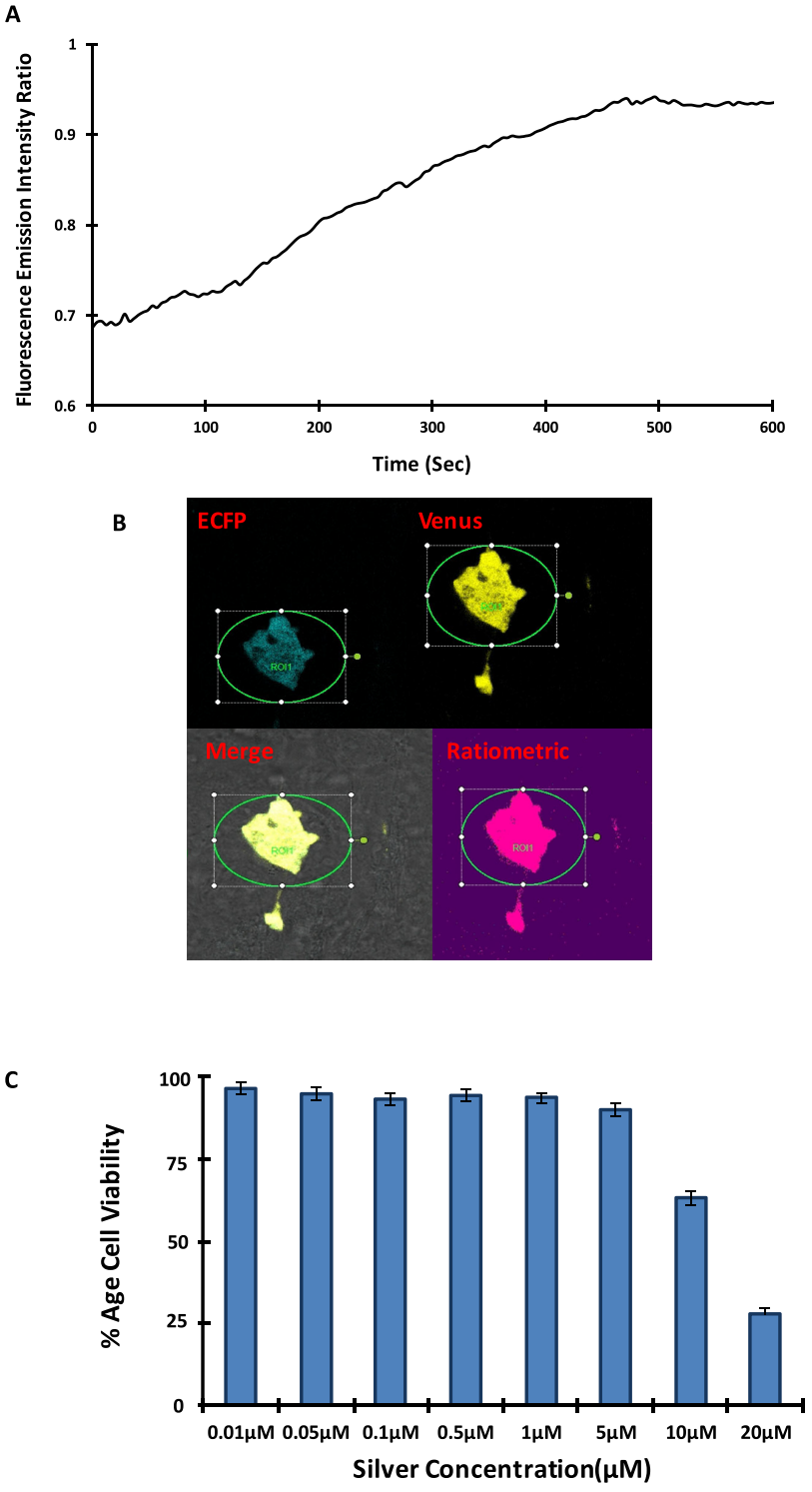

Figure 8. Real-time imaging of SenSil in the HEK-293T cell line. (A) HEK-293T cells were also transfected with SenSil and the emission intensity ratio changes were recorded for the defined period. The graph indicates the Venus/ECFP ratio change for 10 min. (B) Confocal images showing expression of SenSil in the presence of Ag^{+} in the HEK-293T cell line. (C) Cell viability studies of silver ions on HEK-293T. Viability of HEK-293T cells treated with increasing concentrations of Ag^{+} ions (0.01−20 μM) using the 3-[4,5-dimethylthiazol-2-yl]-2,5-diphenyltetrazolium bromide (MTT) assay. Percent cell viability was calculated with respect to the untreated control cells.

(>10 μM), but in the detection range of nanosensor, it is nontoxic to the cells.

3. CONCLUSIONS

FRET-based genetically encoded nanosensors are of current interest to researchers to monitor and measure metabolites in living cells in real time. These nanosensors help us to overcome the limitation of toxicity and delivery problem of chemical dye-based probes. The periplasmic protein *CusF* was successfully converted in to a FRET-based genetically encoded sensor for silver ions. We have developed a simple, sensitive, and selective genetically encoded fluorescence-based biosensor

https://doi.org/10.1021/acsomega.1c00741
ACS Omega 2021, 6, 14164−14173

for real-time monitoring of the level of Ag^+ ions in vitro as well as in eukaryotic and prokaryotic systems. The SenSil analyzed the flux of silver ions in living cells noninvasively. This sensor would be useful to increase our understanding of the regulatory point of the metabolic pathway of silver ion uptake and assimilation.

4. METHODS AND METHODOLOGY

4.1. Designing of the Construct. A cassette was prepared by attaching the donor fluorophore (ECFP) and acceptor fluorophore (Venus) in the pRSET-B vector (Invitrogen, USA). Primers containing restriction sites *Bam*HI at the 5′ end and *Kpn*I sites at the 3′ end along with the flanking bases of the recognition sequences were used for the amplification of ECFP. A similar strategy was followed for amplification of Venus using *Kpn*I and *Hind*III enzyme sites at 5′ and 3′ ends, respectively. The sequence and crystal structure of the *CusF* protein (silver-binding domain) were retrieved from the National Centre for Biotechnology Information (NCBI) database and Protein Data Bank. Signal peptides of 23 amino acids from the N-terminus of the silver-binding protein were identified with the help of Signal P4.1 server (CBS, Denmark). The *CusF* gene sequences were amplified from the genomic DNA of *E. coli* DH10*β* with restriction sites *Kpn*I at both ends. The nanosensor construct was designed by inserting the amplified *CusF* gene between ECFP and Venus and fidelity of the construct pRSET-B-ECFP_*CusF*_Venus was confirmed by full-length sequencing (Figure S1). These sequences were then transferred to the pYES-DEST52 vector (Invitrogen, USA) through the gateway cloning technology using the LR clonase II enzyme following the manufacturer's instructions. *S. cerevisiae*/URA3 strain BY4742 was chosen as the eukaryotic host and transformed with the pYES-DEST-ECFP_*CusF*_Venus sequence. The *S. cerevisiae* strain was maintained on a yeast extract peptone dextrose (YEPD) agar medium and grown in the liquid YEPD medium at 30 °C with aeration in a shaker. The construct was further cloned at *Bam*HI and *Hind*III restriction sites in the eukaryotic expression vector pcDNA3.1 (−) (Invitrogen, USA) to express the sensor protein in HEK-293T cells.

4.2. Expression and Purification of the Sensor Protein. The plasmid pRSET-B-ECFP_*CusF*_Venus was transformed in *E. coli* BL21 Codon Plus competent cells using the heat shock method. For the expression of the nanosensor, protein cells were grown in Luria−Bertani (LB) media at 20 °C at 150 rpm by adding 100 μg/mL ampicillin for 22 h until OD reaches 0.4−0.6. The cells were further induced by 0.5 mM IPTG and allowed to grow for another 20 h in the dark. After 20 h, the cells were harvested using a refrigerated centrifuge (Thermo Scientific, USA) at 4500 rpm for 30 min and the cell pellet was resuspended in 20 mM Tris−Cl (pH 7.8). Cell lysis was performed by ultrasonication (Sonics, USA) for 5−6 min with 15 s pauses. A cell-free lysate was obtained by centrifugation at 4500 rpm for 20 min. The supernatant was transferred to a Ni-NTA resin (Qiagen, Germany) and kept at 4 °C on a rocker shaker for 1 h to allow binding of the His-tagged sensor protein to the resin. The sensor protein was purified by His-binding affinity chromatography (Qiagen, Germany). Washing of the column was done using an ice-cold wash buffer (20 mM Tris−Cl, pH 8.0, 10 mM imidazole), and the sensor protein was eluted with an elution buffer (20 mM Tris−Cl, pH 7.8, 300 mM imidazole). The purified protein was named Sensor for Silver (SenSil) and stored at 4 °C overnight to provide adequate time for proper folding after the purification process.

4.3. In Vitro Characterization of SenSil. *4.3.1. Emission Spectral Analysis of SenSil.* The fluorescence emission spectrum analysis of the purified sensor protein was carried out using a monochromator microplate reader (Synergy H1, BioTek, USA) with and without adding silver ions. The excitation was carried out at 420 nm and the emission fluorescence intensity was registered between 460 and 600 nm.

4.3.2. Testing the pH Stability of SenSil. The kinetics of the nanosensor was initially carried out in various buffer systems, that is, 20 mM PBS, Tris-buffered saline (TBS), and MOPS with changing pH values. The sensitivity of the sensor protein was tested with these buffers over a diverse range of pH values. The isolated sensor protein was diluted 20 times using the respective buffers. In another study, the stability of the sensor protein was tested with the MOPS buffer in the pH range of 5.0−8.0 with the addition of silver and the absence of silver. The ratiometric change was monitored using a microplate reader using an excitation filter of 420/20 nm and the emission filter set for ECFP and Venus was adjusted to 485/20 and 540/20 nm, respectively.

4.3.3. Specificity and Effect of Other Biological Metal Ions. To determine the specificity of SenSil, various metal ions were used. The FRET ratio was recorded after adding 20 μL of Cu^{2+}, Ag^+, Ni^+, Mn^{2+}, and Fe^{2+} metals at six different concentrations, that is,100, 200, and 500 nM and 1, 5, and 10 μM. The potential influence of biologically relevant metal ions such as Ca^{2+}, Mg^{2+}, Na^+, and K^+ on the detection specificity of the nanosensor was also examined. The change in the fluorescence intensity ratio was monitored after addition of 1 μM silver ions.

4.3.4. Saturation Curve and Affinity Mutants. The affinity of the nanosensor was tested by measuring the FRET responses toward increasing concentrations of Ag^+, and the affinity constant (K_d) was calculated by fitting the curve in the binding isotherm

$$S = (r - r_{apo})/(r_{sat} - r_{apo}) = [L]/(K_d + [L])$$

where S is saturation, $[L]$ is the ligand concentration, r is the ratio, r_{apo} is the ratio in the absence of a ligand, and r_{sat} is the ratio at saturation with a ligand determined using GraphPad Prism 7 software. To increase the physiological detection, range of the silver sensor, point mutations were introduced to develop the affinity mutants of the sensor using the QuikChange site-directed mutagenesis kit. Using the data from the crystal structure of *CusF*,[2] two affinity mutants were generated. The mutants were created by substituting the amino acid residues in the binding pocket of the binding protein *CusF*, and histidine was replaced by aspartic acid (H36D) at position 36 and phenylalanine 71 was changed to tryptophan (F71W) (Figure S2). For further analysis, these affinity mutants were expressed and purified as the WT sensor.

4.4. Real-Time Monitoring of Silver in Bacteria and Yeast. Cell-based experiments were performed based on the works of Soleja et al.[30] and Kaper et al.[31] A monochromatic microplate reader was used to quantify the FRET ratio changes from *E. coli* BL21 Codon Plus (DE3) cell suspensions expressing the SenSil. The cells were grown in the LB medium for 3 days at 20 °C in the dark. The bacterial cell suspension (180 μL) was combined with 20 μL of 5 μM Ag^+ ions and dispensed in triplicate in each microplate well. The sensor's response to fluorescence emissions in the form of a FRET

https://doi.org/10.1021/acsomega.1c00741
ACS Omega 2021, 6, 14164−14173

signal was reported at regular intervals of 5 min for a total of 65 min. A confocal microscope (Leica, Wetzlar, Germany) equipped with a confocal head TCS-SPE, a 63× objective piece with 1.53 NA, and a coupled camera was used for checking the expression and to take images of SenSil after fixing the expressed bacterial cells using a medical adhesive on a glass slide.

The sensor protein was expressed into the yeast, and the construct was transferred into the yeast expression vector pYES-DEST52 containing the GAL1 promoter using the gateway technology. *S. cerevisiae*/URA3 strain BY4247 was used and maintained on a SD medium supplemented with 2% sucrose and 3% galactose at 30 °C under aeration on a rotary shaker incubator for 3−5 days. Imaging of the expressed yeast cells was performed using a confocal microscope (Leica DMRE) equipped with a confocal head TCS-SPE (Leica, Wetzlar, Germany). The yeast cells were fixed on the glass slides using a medical adhesive and covered with a poly-L-lysine-coated cover slip. To measure the flux of silver ions in yeast cells, the emission intensity ratio change was recorded using LAS-AF software (Leica, Wetzlar, Germany) with 420/20 nm excitation and two emission filters, that is, 485/20 nm for donor ECFP and 540/20 nm for acceptor Venus. The change in the fluorescence intensity ratio was monitored for 10 min after adding 5 μM Ag^+ ions. The region of interest was chosen to calculate the intensity ratio changes in real time.

4.5. Monitoring of SenSil in HEK-293T Cells. For monitoring the flux of silver ions in mammalian cells, the construct was shuttled into mammalian expression vector pcDNA3.1(−). HEK-293T cells were cultured at 37 °C on a Dulbecco's modified eagle's medium (DMEM, Sigma, USA) with 10% fetal calf serum, 50 μg/mL ampicillin, and 5% CO_2. These cells were plated in 6-well culture plates and transfected with pcDNA-ECFP_*CusF*_Venus using a lipofectamine transfection reagent. For the expression of the nanosensor, cells were grown for 2 days. FRET ratio imaging of HEK-293T cells was performed after 2 days of transfection using a confocal microscope (TCS-SPE, Leica, Germany) with 1.53 NA, 63× oil immersion objective, and a cooled charge-coupled camera.

4.6. Cell Culture and Cytotoxicity Studies. The HEK-293T cell culture was maintained in DMEM supplemented with 10% heat-inactivated FBS and 1% antibiotic−antimycotic cocktail (penicillin, streptomycin, and amphotericin-B) in a humidified CO_2 chamber (5% CO_2, 37 °C). The standard MTT assay was used to evaluate the toxicity level of silver ions. Briefly, the cells (9000−10,000 cells/well) were plated in a 96-well culture plate. Cells were incubated in a CO_2 incubator for 24 h at 37 °C. After 80% of confluency, the old media was removed and the cells were treated with increasing concentrations of silver ions (0−10 μM) for 12 h. The experiment was repeated in triplicate. After incubation, the cells were washed and further incubated for 4−5 h with 100 μL of incomplete DMEM media and 10 μL of MTT solution (taken from 5 mg/mL stock) at 37 °C in the CO_2 incubator. The supernatant media of cells were replaced by 150−200 μL of dimethyl sulfoxide to solubilize the remaining black fuzzy crystals (formazan) on the rocker shaker. Formazan dissolved to give a purple-blue color. After 30 min, the absorbance of the resultant solution was measured at a wavelength of 570 nm using a microplate ELISA reader (Bio-Rad). Finally, the viability of the cells was determined and a graph was plotted against silver ion concentrations.

■ ASSOCIATED CONTENT

Supporting Information

The Supporting Information is available free of charge at https://pubs.acs.org/doi/10.1021/acsomega.1c00741.

NCBI Blast sequencing result of the WT sensor and dendrograms showing confirmation of the mutant variants of SenSil (PDF)

■ AUTHOR INFORMATION

Corresponding Author

Mohd Mohsin − *Department of Biosciences, Jamia Millia Islamia, New Delhi 110025, India*; orcid.org/0000-0002-4127-5970; Phone: +91-(11)26981717; Email: mmohsin1@jmi.ac.in; Fax: +91(11)2698.0229

Authors

Neha Agrawal − *Department of Biosciences, Jamia Millia Islamia, New Delhi 110025, India*

Neha Soleja − *Department of Biosciences, Jamia Millia Islamia, New Delhi 110025, India*

Reshma Bano − *Department of Biosciences, Jamia Millia Islamia, New Delhi 110025, India*

Rahila Nazir − *Department of Botany, Jamia Hamdard, New Delhi 110062, India*

Tariq Omar Siddiqi − *Department of Botany, Jamia Hamdard, New Delhi 110062, India*

Complete contact information is available at: https://pubs.acs.org/10.1021/acsomega.1c00741

Notes

The authors declare no competing financial interest.

■ ACKNOWLEDGMENTS

The first author (N.A.) wishes to express her thanks to the Department of Biotechnology (DBT), Govt. of India for providing Senior Research Fellowship grants. The financial assistance for conducting this research work in the form of a research grant under the nanobiotechnology scheme (no. BT/PR22248/NNT/28/1272/2017) from the Department of Biotechnology, Govt. of India is greatly acknowledged.

■ REFERENCES

(1) Jaishankar, M.; Tseten, T.; Anbalagan, N.; Mathew, B. B.; Beeregowda, K. N. Toxicity, mechanism and health effects of some heavy metals. *Interdiscip. Toxicol.* **2014**, *7*, 60−72.

(2) Kittleson, J. T.; Loftin, I. R.; Hausrath, A. C.; Engelhardt, K. P.; Rensing, C.; McEvoy, M. M. Periplasmic Metal-Resistance Protein CusF Exhibits High Affinity and Specificity for Both CuI and AgI. *Biochemistry* **2006**, *45*, 11096−11102.

(3) Bury, N. R.; McGeer, J. C.; Wood, C. M. Effects of altering freshwater chemistry on physiological responses of rainbow trout to silver exposure. *Environ. Toxicol. Chem.* **1999**, *18*, 49−55.

(4) Krizkova, S.; Adam, V.; Kizek, R. Phytotoxicity of silver ions. *Chem. Listy* **2009**, *103*, 559−568.

(5) Fung, M. C.; Bowen, D. L. Silver products for medical indications: risk-benefit assessment. *J. Toxicol., Clin. Toxicol.* **1996**, *34*, 119−126.

(6) East, B. W.; Boddy, K.; Williams, E. D.; Macintyre, D.; Mclay, A. L. C. Silver retention, total body silver and tissue silver concentrations in argyria associated with exposure to an anti-smoking remedy containing silver acetate. *Clin. Exp. Dermatol.* **1980**, *5*, 305−311.

(7) EPA CASRN. EPA Drinking Water Criteria Document for Silver. *Environ. Prot. Agency* **1989**, *444*, 7440−7444.

(8) Di Vincenzo, G. D.; Giordano, C. J.; Schriever, L. S. Biologic monitoring of workers exposed to silver. *Int. Arch. Occup. Environ. Health* **1985**, *56*, 207−215.
(9) Williams, N.; Gardner, I. Absence of symptoms in silver refiners with raised blood silver levels. *Occup. Med.* **1995**, *45*, 205−208.
(10) Zhou, W.; Ding, J.; Liu, J. 2-aminopurine-modified DNA homopolymers for robust and sensitive detection of mercury and silver. *Biosens. Bioelectron.* **2017**, *87*, 171−177.
(11) Gong, T.; Liu, J.; Liu, X.; Liu, J.; Xiang, J.; Wu, Y. A sensitive and selective sensing platform based on CdTe QDs in the review. *Sens. Actuators, B* **2016**, *223*, 280−294.
(12) Lansdown, A. B. G. A Pharmacological and Toxicological Profile of Silver as an Antimicrobial Agent in Medical Devices. *Adv. Pharmacol. Sci.* **2010**, *2010*, 1−16.
(13) López-López, J. A.; Jönsson, J. A.; García-Vargas, M.; Moreno, C. Simple hollow fiber liquid membrane based pre-concentration of silver for atomic absorption spectrometry. *Anal. Methods* **2014**, *6*, 1462−1467.
(14) Balcaen, L.; Bolea-Fernandez, E.; Resano, M.; Vanhaecke, F. Inductively coupled plasma−Tandem mass spectrometry (ICP-MS/MS): a powerful and universal tool for the interference-free determination of (ultra)trace elements—a tutorial review. *Anal. Chim. Acta* **2015**, *894*, 7−19.
(15) Lai, C. Z.; Fierke, M. A.; da Costa, R. C.; Gladysz, J. A.; Stein, A.; Bühlmann, P. Highly selective detection of silver in the low ppt range with ion-selective electrodes based on ionophore-doped fluorous membranes. *Anal. Chem.* **2010**, *82*, 7634−7640.
(16) Kim, H. N.; Ren, W. X.; Kim, J. S.; Yoon, J. Fluorescent and colorimetric sensors for detection of lead, cadmium, and mercury ions. *Chem. Soc. Rev.* **2012**, *41*, 3210−3244.
(17) Quang, D. T.; Kim, J. S. Fluoro- and chromogenic chemodosimeters for heavy metal ion detection in solution and biospecimens. *Chem. Rev.* **2010**, *110*, 6280−6301.
(18) Li, Y.; Yuan, J.; Xu, Z. A Sensitive Fluorescence Biosensor for Silver Ions (Ag+) Detection Based on C-Ag+-C Structure and Exonuclease III-Assisted Dual-Recycling Amplification. *J. Anal. Methods Chem.* **2019**, 1−8.
(19) Ustimova, M. A.; Lebedeva, A. Y.; Fedorov, Y. V.; Berdnikova, D. V.; Fedorova, O. A. FRET-based metal ion sensing by a crown-containing bisstyryl dye. *New J. Chem.* **2018**, *42*, 7908−7913.
(20) Resch-Genger, U.; Grabolle, M.; Cavaliere-Jaricot, S.; Nitschke, R.; Nann, T. Quantum dots versus organic dyes as fluorescent labels. *Nat. Methods* **2008**, *5*, 763−775.
(21) Kremers, G. J.; Goedhart, J.; van Munster, E. B.; Gadella, T. W. J. Cyan and yellow super fluorescent proteins with improved brightness, protein folding, and FRET förster radius. *Biochemistry* **2006**, *45*, 6570−6580.
(22) Ahmad, M.; Ameen, S.; Siddiqi, T. O.; Khan, P.; Ahmad, A. Live cell monitoring of glycine betaine by FRET-based genetically encoded nanosensor. *Biosens. Bioelectron.* **2016**, *86*, 169−175.
(23) Mohsin, M.; Abdin, M. Z.; Nischal, L.; Kardam, H.; Ahmad, A. Genetically encoded FRET-based nanosensor for in vivo measurement of leucine. *Biosens. Bioelectron.* **2013**, *50*, 72−77.
(24) Loftin, I. R.; Franke, S.; Roberts, S. A.; Weichsel, A.; Héroux, A.; Montfort, W. R.; Rensing, C.; McEvoy, M. M. A Novel Copper-Binding Fold for the Periplasmic Copper Resistance Protein CusF. *Biochemistry* **2005**, *44*, 10533−10540.
(25) Bogner, M.; Ludewig, U. Visualization of arginine influx into plant cells using a specific FRET-sensor. *J. Fluoresc.* **2007**, *17*, 350−360.
(26) Fehr, M.; Frommer, W. B.; Lalonde, S. Visualization of maltose uptake in living yeast cells by fluorescent nanosensors. *Proc. Natl. Acad. Sci. U. S. A.* **2002**, *99*, 9846.
(27) Patel, N.; Gold, M. G. The genetically encoded tool set for investigating cAMP: more than the sum of its parts. *Front. Pharmacol.* **2015**, *6*, 164.
(28) Lansdown, A. B. G. Silver in health care: antimicrobial effects and safety in use. *Curr. Probl. Dermatol.* **2006**, *33*, 17−34.
(29) Arora, S.; Jain, J.; Rajwade, J. M.; Paknikar, K. M. Cellular responses induced by silver nanoparticles: in vitro studies. *Toxicol. Lett.* **2008**, *179*, 93−100.
(30) Soleja, N.; Manzoor, O.; Khan, P.; Mohsin, M. Engineering genetically encoded FRET-based nanosensors for real time display of arsenic (As^{3+}) dynamics in living cells. *Sci. Rep.* **2019**, *9*, 11240.
(31) Kaper, T.; Lager, I.; Looger, L. L.; Chermak, D.; Frommer, W. B. Fluorescence resonance energy transfer sensors for quantitative monitoring of pentose and disaccharide accumulation in bacteria. *Biotechnol. Biofuels.* **2008**, *1*, 11.

https://doi.org/10.1021/acsomega.1c00741
ACS Omega 2021, 6, 14164−14173